PLASMA DYNAMICS

XIX. PLASMA PHYSICS

Academic and Research Staff

Prof. S. C. Brown
Prof. W. P. Allis
Prof. G. Bekefi

Prof. J. C. Ingraham
Dr. G. Lampis

J. J. McCarthy
E. M. Mattison
W. J. Mulligan

Graduate Students

M. L. Andrews
A. J. Cohen
D. L. Flannery
V. G. Forrester, Jr.

E. V. George
P. W. Jameson
R. L. Kronquist
D. T. Llewellyn-Jones
J. E. McClintock

G. L. Rogoff
J. K. Silk
D. W. Swain
J. H. Vellanga

RESEARCH OBJECTIVES

As in the past few years much of our effort continues to be the study of plasma-wave interactions. Most recently, particular emphasis has been placed on the properties of longitudinal electron and ion waves and the effect of plasma inhomogeneities on these oscillations. Many of these studies are made in the regime where the waves are weakly or highly unstable; in the latter situation the plasma may become turbulent and we are looking into methods of studying such turbulent media.

We are continuing our program of developing new plama diagnostic methods of measuring electron and ion densities, temperatures, and distribution of particle velocities. These techniques are based largely on the interaction of transverse electromagnetic waves with the ionized medium. The plasma is either illuminated by radiation of appropriate wavelength and then analyzed, or the noise spontaneously emitted by the plasma is studied. The investigations are made at wavelengths ranging from the visible through the infrared and microwave to the long radio waves. Laser and incoherent sources are used in these studies.

The plasmas used in the aforementioned experiments are made in a variety of ways. In addition to the conventional method of breaking down the gas by DC and RF fields, we ionize the medium by means of a high-powered Q-spoiled laser or by injecting electron beams into a neutral un-ionized gas.

S. C. Brown

A. FAR INFRARED SPECTROPHOTOMETER FOR PLASMA STUDIES

1. Introduction

A double-beam optical-null spectrophotometer is being developed for measuring the absorption of far infrared radiation ($0.1 < \lambda < 1$ mm) by a plasma in order to determine experimentally the plasma mechanisms responsible for the emission of incoherent far infrared radiation. The spectrophotometer operates essentially as follows (see Fig. XIX-1). Two beams of radiation from a far infrared source, S, follow separate optical paths, one beam passing through the plasma, P, the other through a calibrated
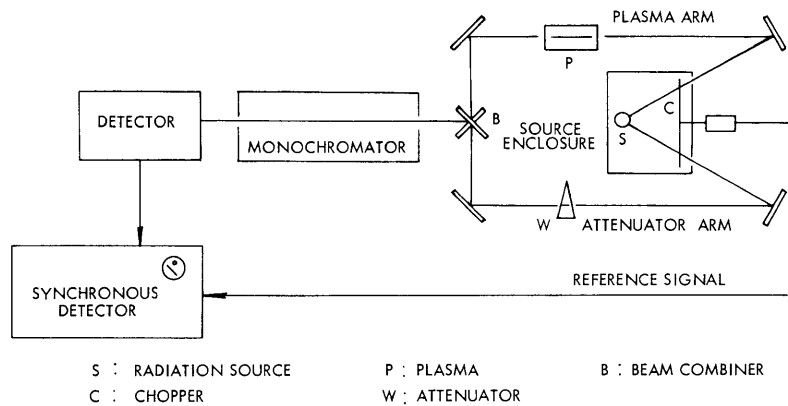
Fig. XIX-1. Schematic illustration of the spectrophotometer.

variable attenuator, W (shown as a movable wedge). The beams are combined at B (by two plane mirrors, one above the other) and are directed to a detector through a grating monochromator, which is set for a particular wavelength. A chopper wheel, C, located near the source permits only one of the beams to pass at a time, effectively switching radiation from S between the two paths at a fixed frequency. A phase-sensitive detector (lock-in amplifier) registers only that part of the detected signal which has this frequency. Thus, the output signal from the synchonous detector corresponds to a difference in the amount of source radiation reaching the detector along the two paths. The attenuator is adjusted to null the detector output, first with the plasma off and then with it on, the difference in attenuator setting in the two cases giving the plasma attenuation.

The relation between attenuator setting and plasma attenuation actually includes the effects of extraneous emission, reflection, and transmission of the various components of the optical system and of its environment, as well as the minimum detectable power of the detection system. If the assumptions are made, however, that all radiation reaching the detector from the chopper plane does so along the intended optical path (that is, stray chopped radiation is negligible), the state of the plasma does not affect the chopped power in either arm, all transmittances in the system (except for the plasma and attenuator) remaining unchanged during the measurement, and the chopped power reaching the detector in either arm is large compared with the minimum detectable power, then the plasma transmittance is given simply by

$$T_p = \frac{T_{wb}}{T_{wa}}. \tag{1}$$

Here T_{wa} is the attenuator transmittance that nulls the detector output with the plasma off, and T_{wb} is the attenuator transmittance that nulls the detector output with the plasma on. Note that the transmittance of the atmosphere and optical components in the

arms need not be equal to make the measurement. They need only remain constant.

The only radiant power, J, that must be considered in determining T_p is that introduced into either beam at the chopper plane, since the synchronous detector responds only to the radiation that is modulated by the chopper. When a chopper blade intersects the beam, J includes radiation from the chopper blade itself, as well as radiation from elsewhere (optical components, plasma, and surroundings) that is reflected into the beam by the blade. When the beam is not obstructed by the chopper, J includes source radiation already attenuated by the mirrors and atmosphere in the source enclosure, radiation from parts of the source enclosure that are now exposed, and radiation from elsewhere that enters the source enclosure and is reflected back out into the beam. For Eq. 1 to hold, care must be taken to insure that, in each beam, the difference between these two power levels with the plasma on is equal to their difference with the plasma off.

2. Optical Arrangement

The optical arrangement has many important features, most of which are concerned with maximizing the radiant flux through the system. This is essential, because of the limited amount of far infrared radiation emitted by the source, S, which is a high-pressure Hg arc lamp. Although, for clarity, much of the following discussion refers to the plasma beam, it is equally applicable to the attenuator beam.

(i) Front-surfaced mirrors are used throughout to avoid the transmission losses and dispersion associated with lenses in the far infrared. The reflectivity of aluminized mirrors is excellent in this spectral region.

(ii) The entire system is designed so that the grating monochromator is the only component that limits the radiant flux through the system. The source is imaged at the monochromator slit. Thus, the grating is the aperture stop of the system and the slit is the field stop. (Note that the monochromator is not overfilled. If it were overfilled, the chopped radiation that misses the grating might reach the detector by an unintended optical path.)

(iii) The radiation beam through the plasma has the smallest possible diameter that is consistent with feature (ii), according to which the monochromator limits the flux through the system. Unfortunately, space does not permit a detailed discussion of this important feature. It turns out that for a plasma length, L, in an ideal optical system, the minimum beam diameter, w, that is consistent with feature (ii) is $w = \sqrt{KL}$, where K is a constant determined by the monochromator dimensions (K = 0.374 cm). This beam diameter is obtained by locating a slit conjugate at one end of the plasma (either end) and a grating conjugate at the other end, with both conjugates being of equal diameter, w. Although the boundaries of this beam are parallel with the optical axis, rays within the beam are at angles θ with respect to the axis up to θ_{max}, given by

tan θ_{max} = w/L. Note that if the plasma tube diameter is smaller than w, the tube itself limits the maximum possible flux through the system. This is an important factor when only weak radiation sources are available, as is the case in the present experiment. (This discussion applies for w ≪ L.)

(iv) To reduce stray chopped radiation, conjugates of both the monochromator slit and grating are located between the source and chopper and apertures of the conjugate dimensions are placed at these locations. These apertures allow only radiation that reaches the real slit and grating by the intended optical path to be chopped. (An ideal optical system is assumed.) Since the beam diameter must have a relative minimum at one member of such a pair of conjugates, one conjugate is small compared with the chopper blade and is located very near the chopper plane to obtain a sharply chopped signal. The other conjugate is large enough to allow for reductions in aperture size without introducing significant diffraction effects.

(v) A beam combiner is located at a grating conjugate just before the monochromator entrance slit. The beam combiner consists of two plane mirrors, one located above the other, each directing one of the two beams into the monochromator. The size of this grating conjugate is large enough to be split conveniently by the two mirrors (with negligible diffraction effects), and it is located relatively close to the monochromator, permitting reasonable flexibility in arranging the remaining mirrors for the two separate beams. (Since there is a focusing mirror between the monochromator and beam combiner, the beam combiner can be located closer to the monochromator if it is located at a grating conjugate rather than at a slit conjugate.) The grating conjugate in the source enclosure is made larger than its corresponding slit conjugate (which is small and near the chopper plane) so that one-half of its aperture may be obstructed, thereby allowing chopped radiation to reach only the half of the beam combiner that directs the radiation into the monochromator. Radiation from one beam that reaches the half of the beam combiner intended for the other beam will be reflected out of the optical path, and may reach the detector by an unintended path (for example, without passing through the monochromator).

(vi) Since high-quality image formation is not of primary importance in the system, spherical mirrors are used for focusing purposes. At all such mirrors the incident and reflected beams are as close to being on-axis as possible.

(vii) The system contains only mirrors that are conveniently available from suppliers' stock, in order to facilitate initial construction, component replacement, and system alterations in the future. It was possible to design the system from a mirror selection with focal lengths 7.5, 10, 15, 20, 30 cm and diameters of 5, 7.5, 10 cm.

(viii) The optical path lengths in the system are limited as much as possible to reduce atmospheric absorption and diffraction losses and to facilitate construction. The system is designed to accommodate an enclosure if purging becomes necessary.

(It may be possible to avoid this necessity by operating at appropriately selected wave-lengths.)

(ix) The system can be operated as a single-beam instrument if in one beam the obstacle over one-half of the grating conjugate in the source enclosure is removed and the beam-combiner mirrors are made parallel to direct that beam into the monochromator. In this case the entire radiant flux is utilized on one arm, rather than being divided between two arms. The other beam should be blocked at the source enclosure, to prevent it from contributing stray chopped radiation to the detector.

(x) The source enclosure openings face away from the monochromator and detector to reduce stray chopped radiation, and the radiation beams intersect the chopper plane and source enclosure face at an angle, so that radiation from components in the system, particularly from the plasma, will not be reflected back into the beam.

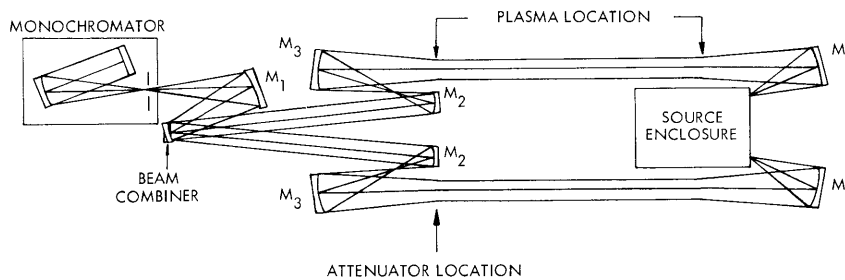Figure XIX-2 illustrates the optical arrangement of the system from the source

Fig. XIX-2.   Optical layout of the spectrophotometer (showing only focusing mirrors).

enclosure to the monochromator. To avoid unnecessary confusion, the plane mirrors that are required are omitted from the illustration. Plane mirrors are used to bend the beam, to insure that the incident and reflected beams at each spherical mirror are as close to being on-axis as possible, and to compress a long beam section into a small space (by "folding" the beam) where this is necessary. The portion of the system between the source and monochromator is illustrated again in Fig. XIX-3 for the plasma arm, where, for simplicity, the mirrors are represented as lenses. The part of the system between the source and beam combiner is duplicated in both beams, with the attenuator being located at σ_p in its arm. In each beam radiation traverses only one-half of each grating conjugate so that at the beam combiner and at the grating itself the two beams are adjacent, one above the other. At the slit and its conjugates following the beam combiner the two beams overlap. Consequently, in double-beam operation each beam contributes one-half of the radiant flux through the monochromator.

The slit and grating conjugates at the plasma ends are arranged as shown so that the
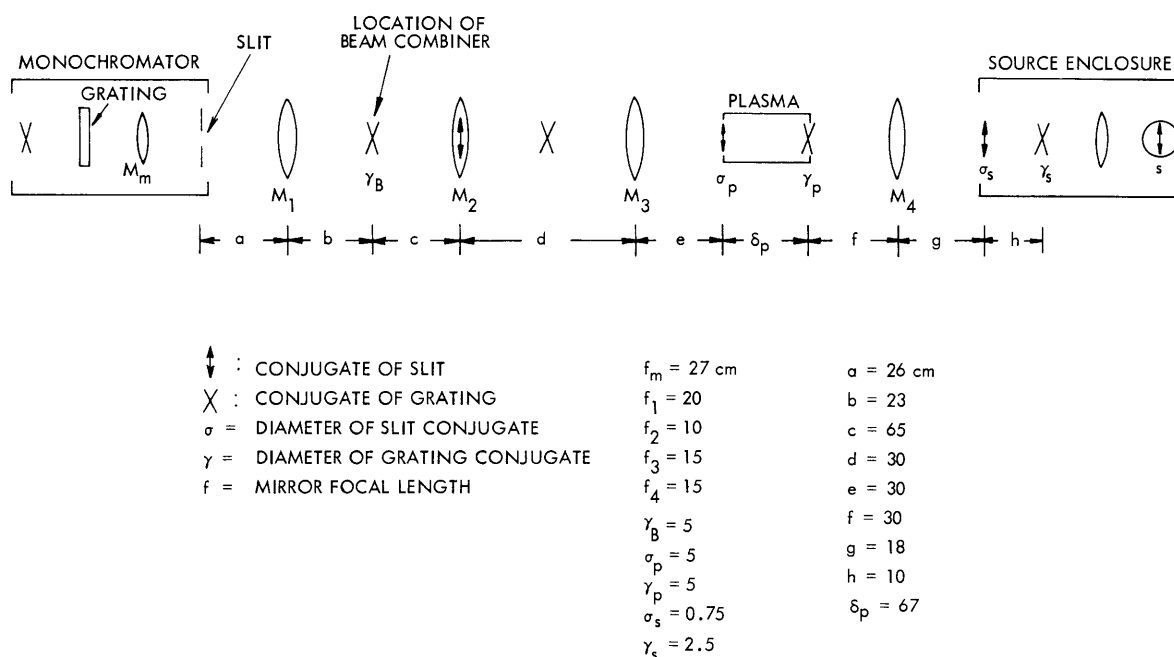
Fig. XIX-3.   Locations of the slit and grating conjugates in the system.

required conjugates in the source enclosure can be obtained with a single concave mirror between the source enclosure and plasma.   This is convenient because the experimental space in this region is limited.

Three concave mirrors (M_1, M_2, M_3) are used between the plasma and the monochromator to produce the required slit and grating conjugates at the plasma ends and at the beam combiner.   The mirror, M_4, was selected to give convenient dimensions between the plasma and the source enclosure apertures, as well as convenient sizes for these apertures. The focal lengths of these mirrors are listed in Fig. XIX-3, along with some calculated system dimensions.   These dimensions actually only approximate the final dimensions of the optical layout, since no attempt was made to account accurately for such things as aberrations or deviations of the actual focal lengths from the expected values.   To adjust for these effects, slight alterations were made experimentally in the dimensions and aperture sizes.

Several different kinds of attenuators are being considered for use in the system. At present, a simple wedge of low-absorption material is being tried.

The monochromator is a Perkin-Elmer prism monochromator (Model 99) that has been modified for use as a single-pass grating instrument.   The f number of this Littrow-type instrument is approximately 3.8.   The slit height is 12 mm, and the maximum slit width has been increased to appoximately 8 mm.

When required, radiation filters (wire-mesh reflection filters) will be located

between the monochromator and detector in order to act on both beams simultaneously. The detector is a Mullard Indium Antimonide photoconducting detector.

The plasma will be a DC discharge (5 cm in diameter, 50 cm long). "Bubble windows"[1] will be on the ends of the plasma tube.

The basic optical system has been completed and tested in a preliminary manner, with very encouraging results.

G. L. Rogoff

References

1. G. L. Rogoff, Quarterly Progress Report No. 82, Research Laboratory of Electronics, M.I.T., July 15, 1966, pp. 114-121.

B. EXPERIMENTAL STUDY OF ELECTRON PLASMA OSCILLATIONS

Observations of microwave scattering from density fluctuations in a beam-plasma have been previously reported,[1,2] and it has been established[2] that the density fluctuations are associated with standing waves along the axis of the plasma column. The experimental study of these waves has continued, and we present in this report the experimentally determined disperison relation for the waves and a measurement of their temporal growth rate.

The experimental geometry is the same as described previously,[2] and is illustrated in Fig. XIX-4. Briefly, the plasma is produced by firing an electron beam into un-ionized
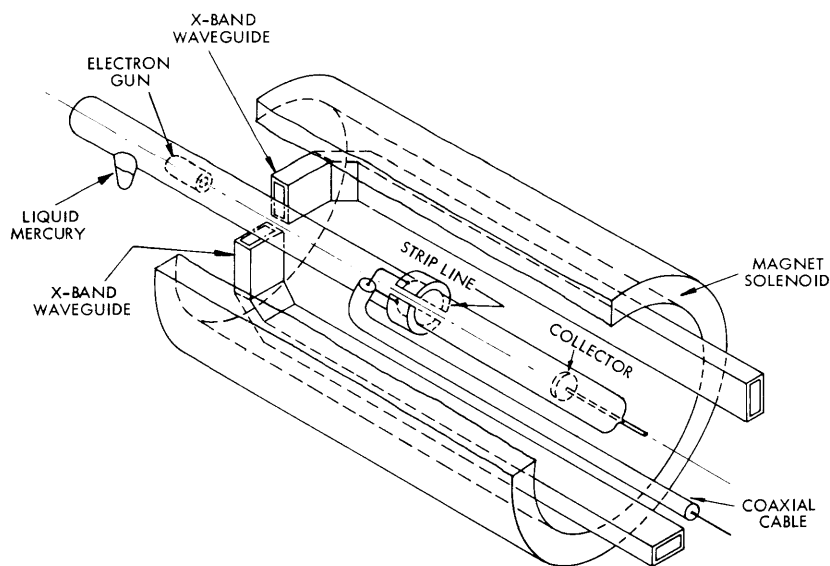

Fig. XIX-4. Experimental geometry.

mercury vapor at a pressure of 2×10^{-4} mm Hg. The axis of the plasma tube is aligned along a uniform magnetic field. Two open-ended pieces of X-band waveguide, which serve as microwave horns in the scattering experiments, and a strip-line antenna, which couples capacitively to the plasma and picks up the oscillations directly, are mounted on a platform that can be moved along the axis of the plasma tube.

The spectra of oscillations at three different axial positions of the strip line are shown in Fig. XIX-5. At each position, peaks occur at the same frequencies, but the
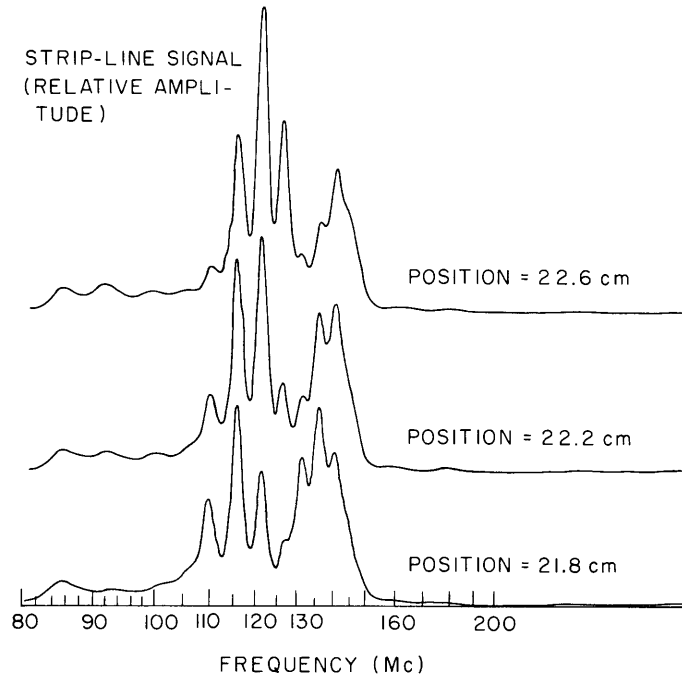

Fig. XIX-5. Amplitude of strip-line signal vs frequency.

relative amplitudes of the peaks are different in each of the spectra. A series of such spectra was taken for axial positions 2 mm apart along the length of the plasma tube which was accessible to the strip line. It was thus possible to follow each frequency peak or mode along the axis and plot its amplitude against distance, as shown in Fig. XIX-6. The minima and maxima, representing nodes and anti-nodes, indicate that each mode can be identified with a standing wave, in which the wavelength is given by twice the distance between two adjacent anti-nodes.

The collector for the electron beam is a helically shaped cathode, which was previously used to run a discharge in the plasma tube. Because of nickel sputtered onto the walls of the tube from this collector cathode, data taken near the collector are not meaningful. Nevertheless, it can be seen from Fig. XIX-6 that for all of the modes shown, the first maximum is spaced almost exactly a half-wavelength from
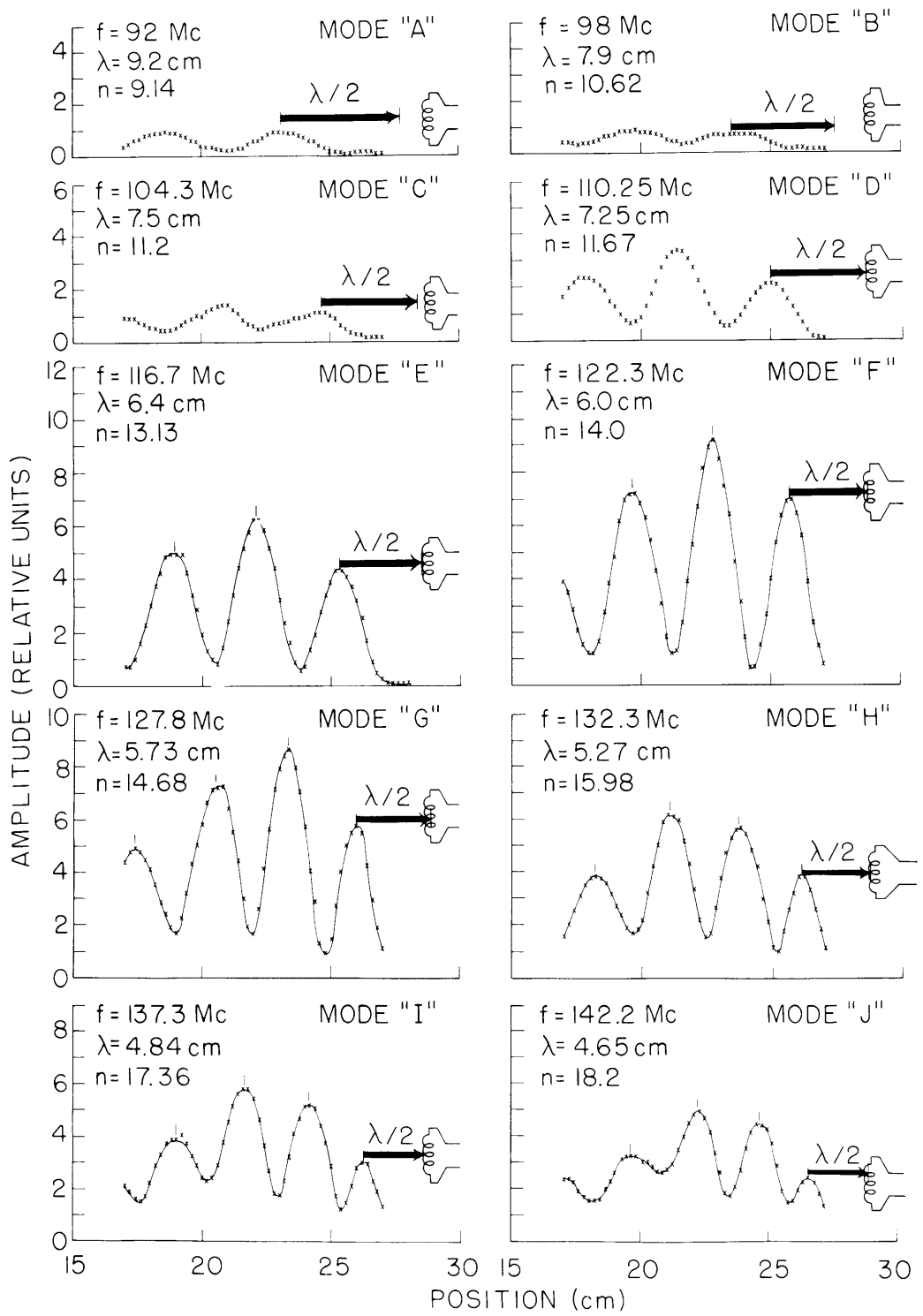
Fig. XIX-6. Amplitude of strip-line signal at fixed frequency vs distance.

the collector. This indicates that the boundary condition at the collector is that it should be an anti-node. This seems reasonable if we assume that the amplitude of the strip-line signal represents the amplitude of the electron density modulation resulting from the wave. The electron density in a plasma wave is roughly analogous to the pressure in an ordinary sound wave in a gas, and for a sound wave the pressure modulation has an anti-node at a rigid end wall. The measurements described above were made with the collector floating, so no current could be drawn, and the analogy of a rigid end wall for a pressure wave seems reasonable. We plan to repeat these measurements with the voltage of the collector variable, to see if the boundary condition of an anti-node at the collector can be changed.

The dispersion relation for the waves can be determined from the set of plots in Fig. XIX-6, since the frequency and wavelength for each mode have been measured. Before plotting the dispersion relation, however, it is interesting to identify with each mode a mode number n, where n is the number of half-wavelengths, $\lambda/2$, along the plasma column of length L = 42 cm. (It is assumed that the electron gun is also at an anti-node.) Therefore, we calculate for each of the modes in Fig. XIX-6 a mode number, $n = 2L/\lambda$, which will be close to, but not exactly equal, an integer, since there is some experimental error in the measurement of λ. From inspection of the n's calculated from Fig. XIX-6, we can identify these modes as corresponding to n = 9, 10, ..., 18. When we plot the dispersion relation, we eliminate the small experimental error in the measurement of λ, by using the λ corresponding to the integral mode numbers instead of the measured λ.

A series of peaks lower in frequency and amplitude than those shown in Fig. XIX-5 were also observed, but their wavelengths were too long to be measured. Nevertheless their mode numbers are known, since the mode numbers of the higher modes have been determined as described above. The dispersion relation is plotted in Fig. XIX-7, where the modes whose wavelengths were measured directly are denoted by x's and the modes whose wavelengths were not measured are denoted by circles.

The straight line in Fig. XIX-7 represents a wave whose phase velocity would be equal to the beam velocity, and it is interesting to note from Figs. XIX-7 and XIX-6 that the waves whose phase velocities are nearest to the beam velocity are most strongly excited. (These are the modes labeled F and G in Fig. XIX-6.) The experimentally determined dispersion relation qualitatively resembles that for plasma waves propagating along the axis of a plasma cylinder with a finite radius,[3] but no comparisons have been made with theory, since measurements have not yet been made of the plasma and electron beam densities.

Additional measurements have also been made of the microwave scattering from these waves. Previously,[2] scattering measurements and direct observations of the waves by means of the strip line were made but not with identical experimental
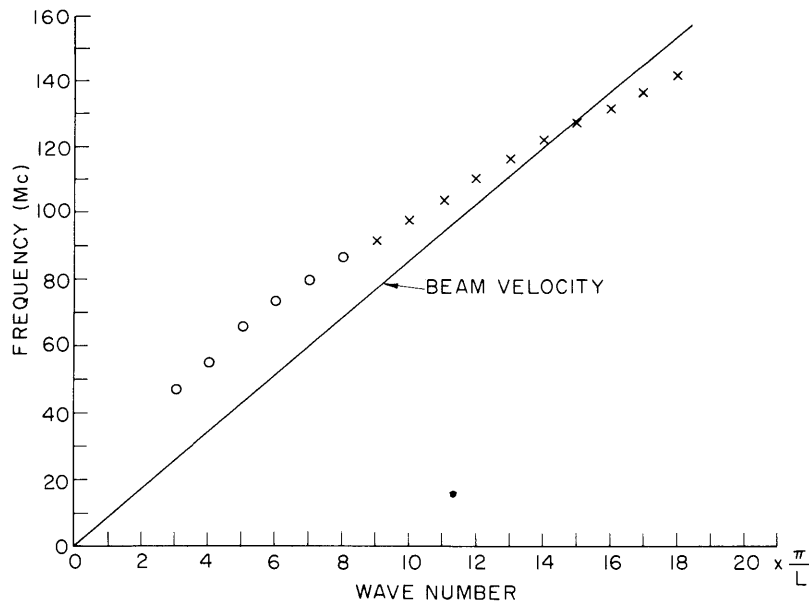
Fig. XIX-7. Frequency vs wave number, $k_n = \frac{n\pi}{L}$.

parameters, so a direct comparison could not be made between the scattering and the strip-line data. The new data are shown in Fig. XIX-8, where we plot on the same graph the direct signal from the antenna against frequency and data points representing
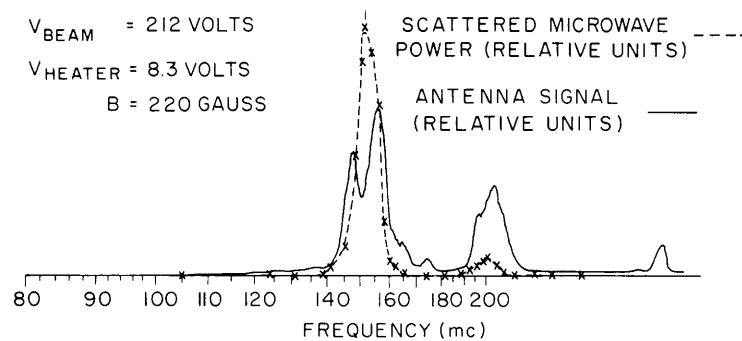

Fig. XIX-8. Antenna signal vs frequency and scattered power vs frequency shift.

the amplitude of the scattered microwave power against frequency shift between incident and scattered frequencies. These data were taken with the microwave horns at the same axial position as the antenna and with identical experimental parameters. The ampli-tudes and shapes of the peaks for the scattering and direct-signal data differ consider-ably, but the frequencies of the peaks coincide quite well. The double peak seen in the

signal picked up by the antenna is not resolved in the scattering data, probably because of the wide bandwidth of the IF strip in the X-band radiometer (10 Mc) as compared with the bandwidth of the radio receiver (2 Mc) which detected the signal from the antenna.

Measurements of the temporal behavior of these waves have also been made. The strip line was connected directly to an oscilloscope and the voltage on the electron gun was pulsed. Figure XIX-9 shows the voltage pulse and the envelope of the signal picked
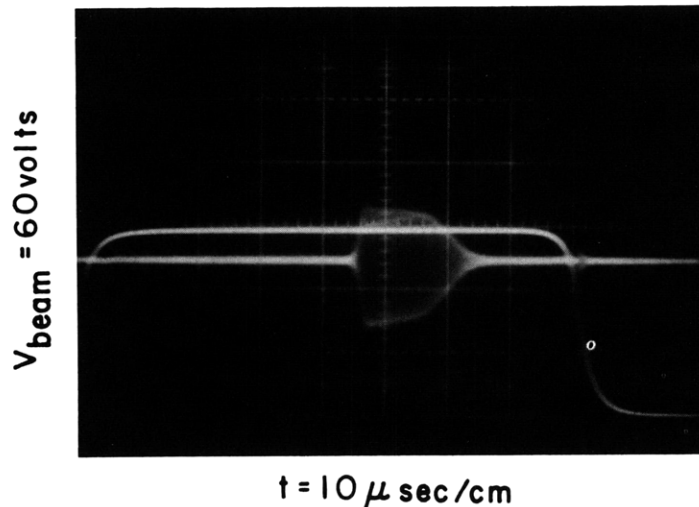

$$t = 10 \, \mu \, \text{sec/cm}$$

Fig. XIX-9. Voltage applied to electron gun and strip-line voltage vs time.

up by the strip line. The oscillations appear approximately 40 µsec after the voltage has been applied to the gun. This time delay may be ascribed to two effects, the time required for the beam to ionize enough neutral atoms so that the plasma frequency reaches the value required for instability, and the time required for the wave to grow from noise to an amplitude that can be detected. It can also be seen that the amplitude of the wave saturates after approximately 2 µsec, and then remains approximately constant for approximately 10 µsec, after which it decays with a longer time constant than that which characterized its growth. It should be noted that the decay begins well before the voltage on the electron gun is turned off. When the pulsewidth was increased, it was found that an instability again appeared several microseconds after the decay of the first instability. This also saturated and decayed and was followed by subsequent bursts of oscillations. Figure XIX-10 shows the growth of the instability shown in Fig. XIX-9, but with an expanded time scale so that both the frequency and the growth rate can be determined. The frequency is 20.7 Mc, which seems to correspond to one of the lower standing-wave modes of the dispersion relation in Fig. XIX-7. The higher modes may correspond to the bursts occurring at later times, but this is not yet clear. The wave
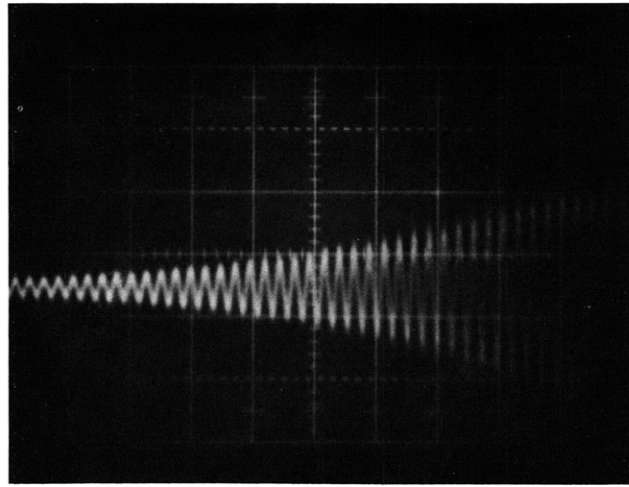
t = 0.2 μsec/cm

Fig. XIX-10.   Strip-line voltage vs time.

amplitude is plotted against time in Fig. XIX-11 on a semi-log scale, and the straight line indicates that the growth is exponential until saturation occurs. The frequency of the wave is $\omega = \omega_r + i\omega_i$, with $\omega_r = 2\pi \times 20.7 \times 10^6$ and $\omega_i = 1.33 \times 10^6$, giving $\omega_i/\omega_r \approx 0.01$. Thus $\omega_i/\omega_r \ll 1$, satisfying a basic assumption of quasi-linear theory which
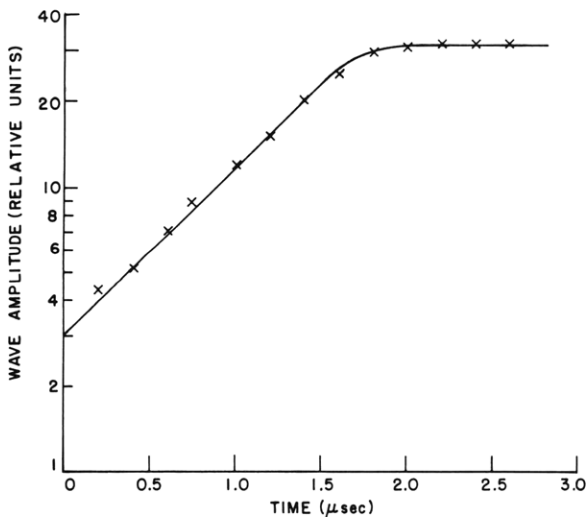

Fig. XIX-11.   Wave amplitude vs time.

describes the saturation of a slowly growing plasma wave by action of the wave back on the electron velocity distribution function. It is hoped that the observed saturation can be explained in terms of this theory.

R. L. Kronquist

References

1. R. L. Kronquist, "Microwave Scattering from an Electron-Beam Produced Plasma," Quarterly Progress Report No. 82, Research Laboratory of Electronics, M. I. T., July 15, 1966, pp. 109-114.

2. R. L. Kronquist, "Microwave Scattering from Standing Plasma Waves," Quarterly Progress Report No. 83, Research Laboratory of Electronics, M. I. T., October 15, 1966, pp. 53-58.

3. A. W. Trivelpiece and R. W. Gould, J. Appl. Phys. $\underline{30}$, 1784 (1959).